Largest explosive eruption in historical times in the Andes at Huaynaputina volcano, A.D. 1600, southern Peru

Jean-Claude Thouret* IRD and Instituto Geofisico del Perú, Calle Calatrava 216, Urbanización Camino Real, La Molina, Lima 12, Perú
Jasmine Davila Instituto Geofísico del Perú, Lima, Perú
Jean-Philippe Eissen IRD Centre de Brest BP 70, 29280 Plouzané Cedex, France

ABSTRACT

The largest explosive eruption (volcanic explosivity index of 6) in historical times in the Andes took place in A.D. 1600 at Huaynaputina volcano in southern Peru. According to chronicles, the eruption began on February 19 with a Plinian phase and lasted until March 6. Repeated tephra falls, pyroclastic flows, and surges devastated an area 70 × 40 km^2 west of the vent and affected all of southern Peru, and earthquakes shook the city of Arequipa 75 km away. Eight deposits, totaling 10.2–13.1 km^3 in bulk volume, are attributed to this eruption: (1) a widespread, ~8.1 km^3 pumice-fall deposit; (2) channeled ignimbrites (1.6–2 km^3) with (3) ground-surge and ash-cloud–surge deposits; (4) widespread co-ignimbrite ash layers; (5) base-surge deposits; (6) unconfined ash-flow deposits; (7) crystal-rich deposits; and (8) late ash-fall and surge deposits. Disruption of a hydrothermal system and hydromagmatic interactions are thought to have fueled the large-volume explosive eruption. Although the event triggered no caldera collapse, ring fractures that cut the vent area point to the onset of a funnel-type caldera collapse.

INTRODUCTION

The largest explosive eruption in historical times in the Andes took place from 19 February to 6 March 1600 at Huaynaputina, a small volcanic center 75 km east of Arequipa in southern Peru (Fig. 1; Thouret et al., 1997). Huaynaputina is not a typical stratovolcano; instead, four vents are nested on the floor (4200 m) of a horseshoe-shaped 2.5 × 1.5 km^2 caldera, open on the east edge of a high volcanic plateau toward the canyon of the Rio Tambo. This caldera breached the summit (4800 m) of the volcano before the A.D. 1600 eruption. The plateau has been built up of no more than 500-m-thick lava flows and ignimbrites of late Miocene to Quaternary age, which overlie sedimentary and intrusive rocks of Mesozoic age.

Repeated tephra falls, pyroclastic flows, and surges buried seven villages, killed ~1500 people (Navarro, 1994), and devastated the landscape within an elliptical area about 70 × 40 km west of the volcano. Pyroclastic flows choked the Rio Tambo canyon and reportedly dammed two temporary lakes (Barriga, 1951). The catastrophic breaching of the lakes released large-scale debris flows that swept down the 120-km-long valley to the Pacific Ocean.

Understanding the voluminous A.D. 1600 Plinian eruption at Huaynaputina is important because of the correlation of a wide spectrum of erupted deposits with reported events, the severe aftermath on the once-populated area around a poorly known volcano, and the probable global climatic impact. This paper shows the large magnitude of the eruption, the variety of the erupted deposits across an area of high relief, and the significance of the event.

LARGE VOLUME AND WIDE SPECTRUM OF TEPHRA

Eight types of erupted deposits encompass an estimated bulk volume of 10.2–13.1 km^3 (Figs. 2 and 3, Table 1).

1. The Plinian pumice-fall deposit was dispersed in a widespread, 1-cm-thick lobe ≥115 000 km^2 to the west and west-northwest toward the Pacific coast (Fig. 2A). According to a log-normal plot of thickness versus the square root of area (Fig. 2B) and to the 360 000 km^2 area of reported ash fall (Fig. 2C), the computed bulk volume of the Plinian fallout is ~8.1 km^3 (dense-rock equivalent [DRE] volume, 4.4–5.6 km^3; Table 1). The tephra is composed of ~80% pumice with rhyolitic glass, 15% crystals (mostly amphibole and biotite), and 5% xenoliths including hydrothermally altered fragments from the volcanic and sedimentary bedrock, and a small amount of accessory lava fragments. The erupted pumice is a white, medium-potassic dacite (average 63.6% SiO_2 and 1.85% MgO) of the potassic calc-alkalic suite. The phenocryst assemblage comprises plagioclase, biotite, amphibole, magnetite, quartz, ilmenite, and apatite. The white color, phenocryst assemblage, and stratigraphic position distinguish the A.D. 1600 tephra from ash from adjacent volcanoes.

2. Three types of nonwelded ignimbrites, 1.6–2 km^3 in volume, are preserved in radial valleys and on the plateau. Lowest in stratigraphic order, an ash-flow deposit is interbedded in the pumice-fall deposit in proximal sections (Fig. 3A). Second, pyroclastic-flow deposits 5–15 m thick above the Plinian fallout are channeled in all catchments and as far as 45 km away from the vent in the Rio Tambo canyon; they are composed of inversely graded pumice lapilli and normally graded vitreous lava clasts in ash, with a few breadcrust bombs (Fig. 3A). Third, thick ash- and pumice-rich pyroclastic-flow deposits,

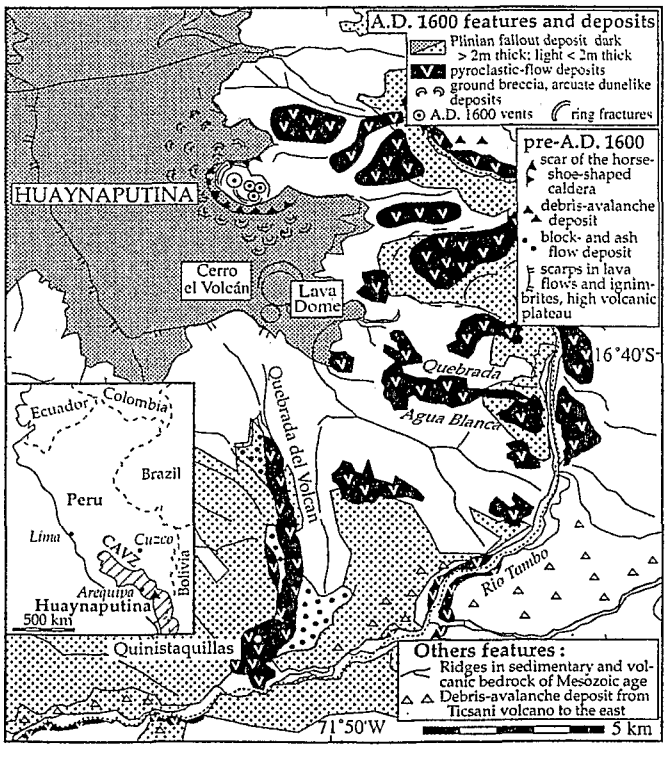

Figure 1. Schematic map of area of Huaynaputina volcano and Rio Tambo area. Inset: Location of Huaynaputina and central Andean volcanic zone (CAVZ) in Peru.

*E-mail: jct@geo.igp.gob.pe.

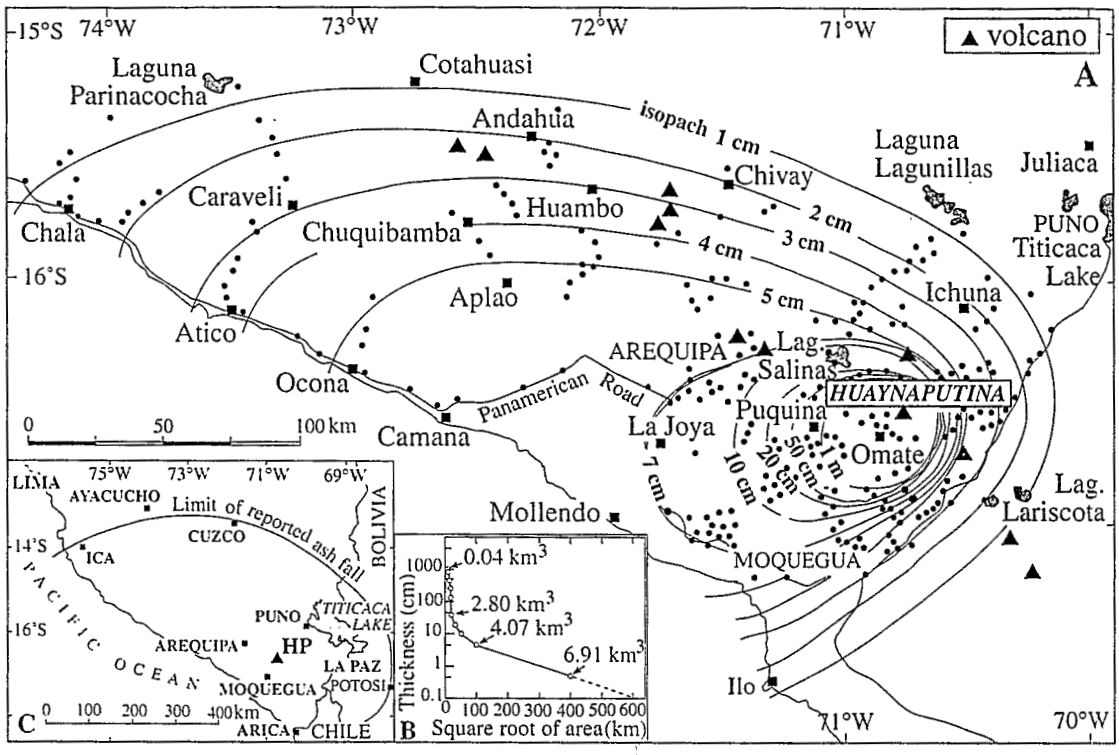

Figure 2. A: Map showing extent and isopachs (thickness in centimeters) of A.D. 1600 Plinian tephra fall from Huaynaputina (HP). B: Plot of thickness vs. square root of area (after Pyle, 1989) for computing bulk volume of Plinian tephra-fall deposit: 6.91 km³ within 1 cm isopach and 8.12 km³ within limit of reported ash fall, shown in sketch map C.

preserved on the plateau, are underlain by crescent-shaped dunes as far as 1.5 km from the caldera rim (Fig. 1). The dunes consist of breccia, a mixture of lava clasts, pumiceous and porphyritic dacite lumps, and xenolithic blocks.

3. One-decimeter- to several-decimeters-thick ash and pumice deposits, fine grained and with few lithic fragments, underlie most of the pyroclastic-flow units in proximal valley sections (Fig. 3A). The sandwave facies and cross-bedded beds as well as the pinch-and-swell and dunelike features point to ground-surge deposits. Other thin, fine-ash layers from ash-cloud surges overlie the pyroclastic-flow units (deposit 3, Fig. 3A).

4. Several massive ash layers totaling 5–20 cm in thickness mantle the pumice-fall deposit as far as 75 km away from the vent (Fig. 3B). They consist of fine ash alternating with coarse ash and lapilli. Both thickness and grain size of the ash layers increase toward the valley-confined ignimbrites.

5. Cross-bedded ash and pumice deposits, 1–3 m thick and showing sandwave facies, accretionary lapilli, and soft deformation, are interbedded in the middle part of the ignimbrite sequence as far as 15 km from the vent in the Rio Tambo valley and tributaries (Fig. 3A). The base-surge

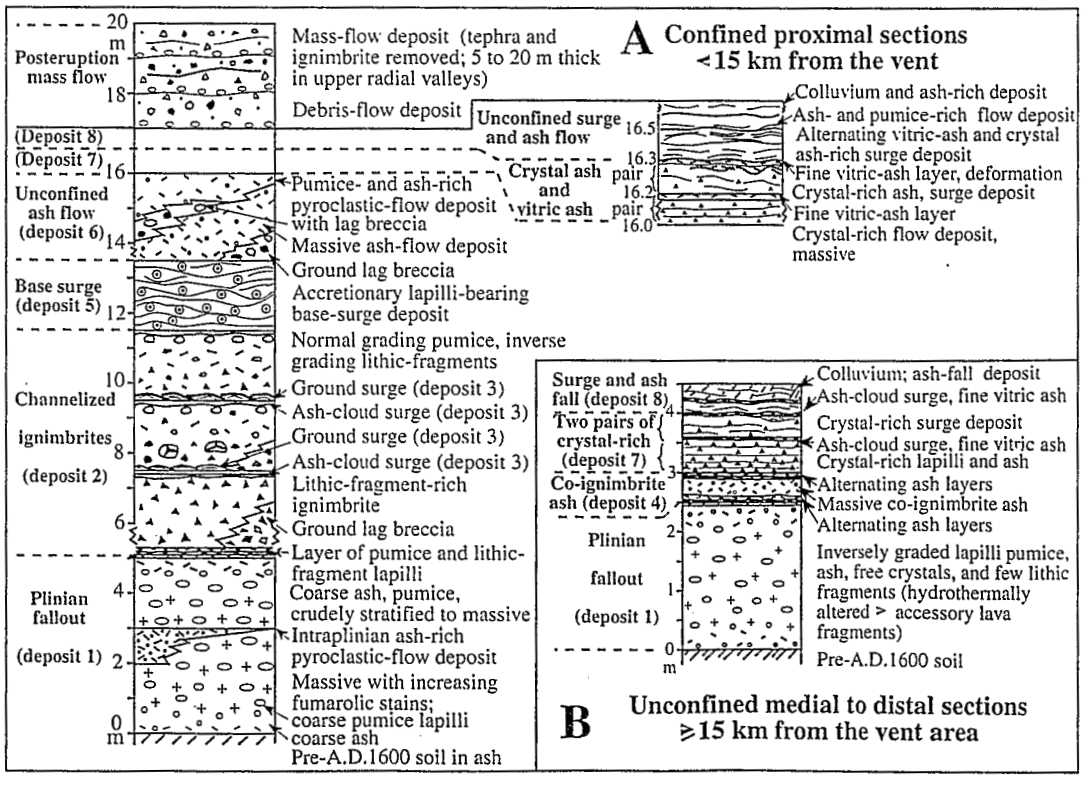

Figure 3. Composite stratigraphic sections of tephra from A.D. 1600 eruption. Deposits numbered 1 to 8 are described in text.

deposits of phreatomagmatic origin represent an estimated volume of 0.05 km^3.

6. Unconfined ash-flow deposits 2–3 m thick in proximal areas (Fig. 3A) correlate with a massive vitric-ash layer 3–4 cm thick as far as 70 km west-northwest of the vent. The flows that emplaced the ash-flow deposits must have surmounted the 2400-m-high left wall of the Rio Tambo canyon 15 km away from source toward the southeast and a series of 1000- to 1400-m-high topographic barriers at least as far as 60 km to the west.

7. A gray, crystal-rich deposit, 15–35 cm thick in proximal to medial sections and 0.5–0.6 km^3 in volume, overlaps a large part of the area mantled by the Plinian fallout as far as 75 km west-northwest of the vent. The crystal-rich deposit, thicker on slopes that face the vent, is interbedded between ash-flow deposits 6 and 8 in confined sections (Fig. 3A) or between the deposits 4 and 8 in unconfined sections (Fig. 3B). Crystals of plagioclase, amphibole, biotite, and quartz make up 80% of deposit 7, which is composed of two units separated by a thin fine-ash layer. On ridges as far as 25 km from the source, the upper crystal-rich unit forms cross-stratified dunes.

8. On top of the tephra sequence (Fig. 3B), a 10–30-cm-thick unit of massive, coarse ash is mixed with soil and/or colluvium on slopes. Thin layers of coarse-ash deposit form dunelike features with planar beds on ridges 15–45 km away from the vent.

TABLE 1. VOLCANOLOGICAL DATA FOR A.D. 1600 PLINIAN ERUPTION

Extent of the Plinian fallout (within 1 cm isopach)	≤ 115 000 km^2
Extent of reported ash and dust fallout (Fig. 2C)	~360 000 km^2
Volume of Plinian ejecta (within 1 cm isopach and from Fig. 2C)	~6.9 and 8.1 km^3
Minimum volume percent beyond 1 cm isopach	17.5%
Minimum volume DRE (80% pumice, average density 1.5 g/cm^3)	4.4–5.6 km^3
Minimum volume of lithic fragments	1.05 km^3
Minimum volume of magma	3.75–4.25 km^3
Duration of the Plinian phase	13–19 h
Mass eruption rate (19 h average, DRE magma density 2.4 g/cm^3)	$1.3–1.5 \cdot 10^5$ kg/s
Volumetric eruption rate (same characteristics as above)	$7.0–7.7 \cdot 10^4$ m3/s
Peak mass eruption rate*	$1–2 \cdot 10^8$ kg/s
Column height*	33–37 km
Peak wind velocity*	10–20 m/s
Weight percent ejecta <1mm (at 0.1 T thickness and 0.01 T maximum)	73.5%, 98.3%
Weight percent ejecta <63 μm (at 0.1 T and 0.01 T maximum)	57.6%, 93.4%
Tropospheric injection	Substantial
Stratospheric injection (inferred from ice cores and tree-ring chronology)	Definite
Volume of pyroclastic-flow deposits	1.6–2 km^3
Minimum travel distance of channeled pyroclastic flows, Rio Tambo valley	45 km
Minimum travel distance of ash flows over topographic Barriers	60 km
Volume of pyroclastic-surge deposits	≤ 0.05 km^3
Volume of crystal-rich deposits	0.5–0.6 km^3
Volume of co-ignimbrite ash and/or co-Plinian ash	1.2–2.4 km^3
Total bulk volume (Plinian and post-Plinian tephra)	~10.2–13.1-km^3
Total volume DRE	~6–8.8 km^3
Volcanic explosivity index	~6

*From Sparks (1986) and Carey and Sparks (1986).

EMPLACEMENT OF DEPOSITS AND ERUPTION MECHANISMS

According to chronicles (Barriga, 1951; Vasquez de Espinosa, 1942; Mateos, 1944), the eruption began on 19 February 1600 following four days of intense seismic activity and lasted until 6 March. Correlating historical accounts to measured tephra and inferred eruptive processes, we distinguish five eruptive phases.

Plinian Phase and Dynamics of the Eruption Column

The Plinian phase lasted 13 to 19 h (between 5 P.M. on February 19 and 5 A.M. to midday on February 20) (Barriga, 1951) and delivered the widespread pumice fallout at the onset of the eruption. By using characteristics of the Plinian fallout (Fig. 4) and Carey and Sparks's method (1986), we computed a 33–37-km-high eruption column and a high discharge rate (Table 1). The wide dispersal of tephra across a distance of ~600 km toward the west and west-northwest (Fig. 2A) is due to the pattern of wind directions prevailing from December to March in southern Peru.

The eruption column rapidly became high and sustained, for coarse grain size and reverse grading appear as low as in the first decimeter above the base of the deposit (Fig. 3). An umbrella and/or a shift in wind direction developed only during the second half of the Plinian phase, as demonstrated by the abrupt increase in pumice size in the middle part of the medial sections and by the coarser pumice-fall deposit that directly rests on the pre–A.D. 1600 soil in upwind sections. The high column remained sustained almost throughout the Plinian phase, for the mean size of the pumice decreases only in the uppermost 10 cm of the tephra-fall deposit. The intra-Plinian flow deposit in the middle of the sections in the Rio Tambo valley (Fig. 3A) shows that the eruption column was unstable toward the second half of the Plinian phase. The flow deposit correlates stratigraphically with the increase in hydrothermally altered lithic fragments in the pumice-fall deposit, indicating either vent erosion, higher mass eruption rate, or instability due to local overloading of the column or increased water input.

A hydrothermal system was probably depressurized and fragmented during the Plinian phase, evidenced by (1) the abundance of hydrothermally altered lithic fragments from the base to the middle part of the pumice-fall sections and (2) fumarolic stains coating lithic fragments and pervading pumice. Lithic-rich units with oxidized boulders in the second half of the near-vent Plinian fallout indicate that the conduit walls widened in the hydrothermally altered host rocks during the second part of the Plinian phase. From the drastic decrease in the amount of the hydrothermal component upward in the Plinian fallout, we infer that the flaring process stopped just before the end of the Plinian phase.

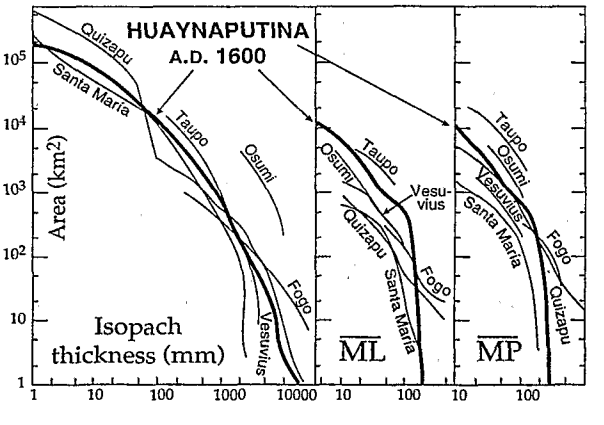

Figure 4. Areas (in square kilometers) enclosed by isopachs and isopleths of maximum pumice (MP) and maximum lithic fragments (ML) sizes (in millimeters) of A.D. 1600 Plinian tephra-fall deposit, for comparison with six well-characterized Plinian eruptions, all referenced in Hildreth and Drake (1992, their plot on p. 111).

Ignimbritic Phase

Following a lull, the explosive activity increased during February 24–27, when earthquakes shook down the cathedral of Arequipa. The increase may correspond to the emplacement of the 1.6–2 km^3 channelized ignimbrites, underlain by and interspersed with ground- and ash-cloud surges (deposits 2 and 3, Fig. 3A).

The ignimbrite-forming eruptive phase tapped another magma batch, as shown by the more evolved composition of the porphyritic, crystal-rich pumice of the ignimbrites: they are more porphyritic, richer in silica (average 65.2% SiO_2), and poorer in magnesium (average 1.72% MgO) than the pumice from the Plinian fallout. Post-Plinian flows, first lithic rich and then pumice and ash rich, deposited a significant volume of ignimbrites (Table 1), whose lack of either welding or gas pipes suggests that the magma was neither very hot nor gas rich. The lithic-rich ignimbrite, channelized in the Rio Tambo valley and tributaries, also deposited ground breccias that formed crescent-shaped dunes on near-vent slopes 1.5 km from the caldera rim.

The massive ash layers (deposit 4) in distal areas >45 km away from source (Fig. 3B) are interpreted as co-ignimbrite ash, although some of the ash layers may have been emplaced by ash falls from a dwindling eruption column during the events recorded on February 20–22. The wide extent (Fig. 2) and the 1.2–2.4 km^3 volume of co-ignimbrite ash and co-Plinian ash are consistent with contemporary reports that ash fell repeatedly on Arequipa during the two weeks after the Plinian phase.

Hydromagmatic Phase

Four additional events occurred from February 28 to March 2. Of these, one or two may correspond to the hydromagmatic phase, which emplaced base surges interbedded in the ignimbrite sequence. Evidence for repeated hydromagmatic explosions includes accretionary lapilli and soft deformation in base-surge deposits and breadcrust bombs in ignimbrites and ground breccia. This evidence suggests that magma-discharge decreased because the vent area widened owing to catastrophic erosion concomitant with the eruption of lithic-rich ignimbrites. The hydromagmatic component and the base-surge deposits point to an explosive episode that likely opened the three funnel-shaped vents now in the pre–A.D. 1600 caldera.

Phase of Emplacement of Crystal-Rich Flow and Surge Deposits

Of the four events of February 28 to March 2, at least two violent explosions likely released the two crystal-rich layers of deposit 7 (Fig. 3A). Each crystal-rich flow and surge deposit and its overlying vitric ash form a genetically related pair: the percentage of crystals in the crystal-rich deposit and the thickness of each vitric-ash layer both increase away from source. The related pair suggests that the crystal enrichment through density segregation and elutriation of vitric-fine ash occurred during the flow transport over the rugged topography. The crystal-rich deposit implies that an originally crystal-rich magma was tapped toward the end of the eruption, a fact that is reflected by the increase in density and crystal content of the pumice throughout the erupted sequence.

Phase of Emplacement of Ash Flows and Surges

Intermittent ash falls that reportedly continued in Arequipa from February 28 to at least March 6 may have derived from ash flows and surges that left deposits 6 and 8 at top of sections (Fig. 3). Unconfined ash-flow deposits traveled more than 60 km over a relief of six ridges 1000 to 1400 m high above valley floors and normal to flow direction. The equation $v = \sqrt{gh}$, where g = force of gravity, h = height of the topographic barriers, and v = velocity, produces a minimum ash-flow velocity of 50 to 110 m/s. The rugged topography and high relief controlled the flow transport and deposition: massive ash-flow deposits on ridges change laterally to bedded surge deposits.

Posteruption Emplacement of Mass-Flow Deposits

According to Barriga (1951), the sky remained hazy until April 2 when the air eventually cleared, but Mateos (1944) and Ocaña (1969) stated that dust remained in the air for nine months, a fact that we attribute to the emplacement of voluminous, posteruption mass-flow deposits. Reworked ignimbrite and debris-flow deposits 5–20 m thick (Fig. 3A) mantle the edges of the plateau and are channeled as far as 15 km away in the radial valleys.

SIGNIFICANCE OF THE ERUPTION

Such a voluminous explosive eruption (Table 1) occurred at this site because of the disruption of a hydrothermal system during the Plinian phase and because of hydromagmatic interactions interspersed in the eruptive sequence. Does this event represent the onset or the end of a long-lasting process? Two preliminary clues are available.

First, the horseshoe-shaped caldera had already breached the stratovolcano and had been modified by earlier eruptions. The A.D. 1600 eruption blew away domes that had previously grown in the area, led to the formation of the crater complex (Fig. 1), but induced no debris avalanche: the Plinian fallout rests on a thin soil above the weathered top of older debris-avalanche deposits and pyroclastic deposits that fill the Rio Tambo valley (Fig. 1). A pumice-fall deposit interbedded in the pyroclastic deposits correlates with a similar pumice-fall deposit from Huaynaputina that yielded a radiocarbon age of 9700 ± 190 yr B.P. (Juvigné et al., 1997).

Second, no caldera formed despite the total 6–8.8 km^3 DRE volume of erupted tephra (Table 1). The lack of caldera collapse may be due to the lithologic behavior of the bedrock relative to the small, eroded Huaynaputina stratovolcano. But ring fractures that cut the vent area point to a funnel-shaped structure beneath the crater complex and to the onset of a funnel-type collapse (Fig. 1).

These clues suggest that the A.D. 1600 eruption may have been a single event in a longer process. Should an eruption of this magnitude occur again in southern Peru, fallout, pyroclastic flows, and surges would wreak havoc in an area where ~30000 people are now directly at risk and would affect the ~700000 inhabitants of Arequipa.

ACKNOWLEDGMENTS

This research was supported by the Institut de Recherche pour le Développement (IRD) and the Instituto Geofísico del Perú (IGP). We thank J.-L. Bourdier and S. Young for improving an early manuscript and R. Waitt for a constructive review.

REFERENCES CITED

Barriga, V. M., 1951, Los terremotos en Arequipa (1582–1868): Arequipa, La Colmena, 426 p.

Carey, S., and Sparks, R. S. J., 1986, Quantitative models of the fallout and dispersal of tephra from volcanic eruption columns: Bulletin of Volcanology, v. 48, p. 109–126.

Hildreth, W., and Drake, R. E., 1992, Volcan Quizapu, Chilean Andes: Bulletin of Volcanology, v. 54, p. 93–125.

Juvigné, E., Thouret, J.-C., Gilot, E., Gourgaud, A., Legros, F., Uribe, M., and Graf, K., 1997, Etude téphrostratigraphique et bioclimatique du Tardiglaciaire et de l'Holocène de la Laguna Salinas, Pérou méridional: Géographie Physique et Quaternaire, v. 51, p. 219–231.

Mateos, F., 1944, Historia general de la Compañía de Jesus en la provincia del Perú: Madrid, Consejo Superior de Investigaciones Científicas, 240 p.

Navarro, R., 1994, Antología del valle de Omate: Arequipa, Universidad Nacional San Agustin, 76 p.

Ocaña, D. de, 1969, Un viaje fascinante por la America Hispana del Siglo XVI: Madrid, Edición A. Alvarez, Historia 16, 256 p.

Pyle, D. M., 1989, The thickness, volume, and grainsize of tephra fall deposits: Bulletin of Volcanology, v. 51, p. 1–15.

Sparks, R. S. J., 1986, The dimensions and dynamics of volcanic eruption columns: Bulletin of Volcanology, v. 48, p. 3–15.

Thouret, J.-C., Davila, J., Rivera, M., Eissen, J.-Ph., Gourgaud, A., Le Pennec, J.-L., and Juvigné, E., 1997, L'éruption explosive de 1600 au Huaynaputina (Pérou), la plus volumineuse de l'histoire dans les Andes centrales: Comptes-Rendus Académie des Sciences Paris, Elsevier, v. 325, p. 931–938.

Vasquez de Espinosa, A., 1942, Compendium and description of the West Indies (translated by C. U. Clark): Smithsonian Miscellaneous Collection, v. 102, 862 p.

Manuscript received September 25, 1998
Revised manuscript received January 14, 1999
Manuscript accepted February 1, 1999